Appendix C

FITTING SANS DATA FROM COIL-LIQUID CRYSTALLINE DIBLOCK COPOLYMER SOLUTIONS

C.1 Appendix

Small-angle neutron scattering (SANS) data from solutions of diblock copolymers having a side-group liquid crystal polymer (SGLCP) block and a random-coil polymer (polystyrene, PS) in a small-molecule liquid crystal (LC) solvent is presented in Chapter 3. The diblock copolymers self-assemble in LC solvent to form micelles composed of PS-rich cores surrounded by SGLCP-rich coronas. Extensive efforts were made to fit the SANS data to structural models in order to extract parameters such as the core radius, the corona thickness, and the aggregation number, but the results are inconclusive. This appendix details the successes and failures of the data-fitting methods used.

C.1.1 Theory of Scattering from Block Copolymer Micelles

The differential scattering cross-section, $\partial\Sigma/\partial\Omega(q)$, from a solution of N mondisperse, spherically symmetric particles of volume V and with neutron scattering contrast $(\Delta\rho)^2$ is given by the product of a form factor, $P(q)$, and a structure factor $S(q)$:

$$\frac{\partial\Sigma}{\partial\Omega}(q) = N(\Delta\rho)^2 V^2 P(q) S(q), \tag{C.1}$$

where $q = 4\pi/\lambda \sin(\theta_s / 2)$ is the magnitude of the scattering vector at an angle, θ_s.[1, 2] The form factor accounts for intra-particle scattering and depends on the shape and composition of the particle. The structure factor accounts for interference between particles and depends on the inter-particle potential. In the case of a solution of polydisperse, interacting particles, a decoupling approximation[3] may be used to write the scattered intensity

$$\frac{\partial \Sigma}{\partial \Omega}(q) = N(\Delta\rho)^2 V^2 P(q)[1 + \beta(q)(S(q) - 1)], \tag{C.2}$$

where $\beta(q)$ is a factor between 0 and 1 that dampens the structure factor oscillations. Interparticle interference becomes negligible when the volume fraction of particles is very small or when particles are correlated on length scales much larger than q. In this case, $S(q) = 1$ and the differential scattering cross-section from a solution of uncorrelated particles, whether monodisperse or polydisperse, is simply

$$\frac{\partial \Sigma}{\partial \Omega}(q) = N(\Delta\rho)^2 V^2 P(q). \tag{C.3}$$

Numerous form factors are available for modeling block copolymer micelles with varying levels of structural detail (Figure C.1). In the simplest case, a micelle may be modeled as a spherical core of homogeneous scattering length density surrounded by a concentric shell of homogeneous scattering length density (Figure C.1a).[4, 5] This model is extended to anisotropic micelles by using ellipsoidal or cylindrical cores and shells, for examples (Figure C.1b,c).[5] More detailed models take into account the polymeric nature of the material in the shell and treat the micelle as a homogeneous core with chains attached to the surface (Figure C.1d)[6, 7] or account for a radial density profile of the polymer in the shell (Figure C.1e).[8-10] These models are extended to anisotropic micelles, as well.[11] Choosing a very detailed form factor can yield more structural information about the micelles, but it also introduces an increasing number of fitting parameters and requires increasingly high-resolution scattering experiments to be confident in the physical significance of the resulting fit. In practice, one narrows the field to physically realistic form factors for the system of interest then chooses the simplest one that can be used to fit the data with consistency between different samples.

The structure factor most commonly employed for block copolymer micelles is the Percus-Yevick model for hard spheres[12, 13] because fits to SANS data are usually equally good regardless of the interparticle potential invoked.[5] For example, Castelletto, Hamley, and Pedersen[14] found that highly swollen micelles formed the BCC lattice expected for soft spheres, but the scattering was equally well modeled with the hard-sphere structure factor as with the soft-sphere structure factor. The Percus-Yevick model is, therefore, preferred because it is one of the few structure factors that can be calculated analytically, thus saving computing time.

Polydispersity of particle size and the limitations of instrumental resolution[15] cause smearing of the intensity profile, and these effects must be accounted for when modeling experimental data. The distribution of block copolymer micelle radii, R, is typically modeled with a Schultz distribution:[3, 4]

$$n(R) = \frac{\left(\frac{\mu+1}{\langle R\rangle}\right)^{\mu+1} R^{\mu} \exp\left[-\left(\frac{\mu+1}{\langle R\rangle}\right)R\right]}{\Gamma(\mu+1)} \qquad \text{(C.4)}$$

$$\mu = \frac{\left(1-\beta^2/\langle R\rangle^2\right)}{\beta^2/\langle R\rangle^2},$$

where n is the population of micelles with radius R, $\langle R\rangle$ is the average radius, β is a width parameter, and Γ denotes the gamma function. Applying this distribution to the differential scattering cross-section from uncorrelated micelles (Equation C.3) gives:

$$\frac{\partial\Sigma}{\partial\Omega}(q) = \int_0^{\infty} n(R)N(\Delta\rho)^2V^2P(q,R)dR\,; \qquad \text{(C.5)}$$

higher-order corrections must be made when $S(q) \neq 1$.[3, 5] The instrument used to measure the scattering pattern has a particular resolution function, $\sigma(q)$, that must be applied to simulate experimentally measured data. The resolution-smeared differential scattering cross-section, $\partial\Sigma/\partial\Omega(q)_{smeared}$, is

$$\frac{\partial \Sigma}{\partial \Omega}(q)_{smeared} = \frac{\int_0^\infty \frac{\partial \Sigma}{\partial \Omega}(q')\exp\left[-\frac{(q'-q)^2}{2\sigma(q)^2}\right]dq'}{\int_0^\infty \exp\left[-\frac{(q'-q)^2}{2\sigma(q)^2}\right]dq'}. \quad \text{(C.6)}$$

C.1.2 Fitting Scattering Data from PS-SGLCP Diblock Copolymer Micelles with the Spherical Core-Shell Form Factor Including Polydispersity and Instrumental Smearing

In practice, the experimentally measured intensity, $I(q)$, is not necessarily in absolute units. $I(q)$ is assumed to be proportional to $\partial\Sigma/\partial\Omega(q)$ and the proportionality constant is lumped together with the product $N(\Delta\rho)^2V^2$ into an overall multiplicative factor, K. Physical parameters are extracted from the data by hypothesizing a form factor and structure factor then using least-squares algorithms to determine the model parameters that give the best fit to the experimental data.[5]

The structure factor was found to make a negligible contribution to the scattering from coil-SGLCP diblocks dissolved in LC solvent. The peaks often observed at low q are insensitive to concentration, in opposition to the strong concentration dependence predicted by the hard-sphere structure factor model. Indeed, in a series of diblock solutions ranging from 2 to 20 wt % polymer, the peak positions do not change with concentration and the maximum intensity (normalized by concentration) varies by less than 40%, implying that $S(q)$ is, at most, 1.4.[16] These structure factor contributions are ignored and scattering patterns are modeled as the product of a form factor and a multiplicative constant.

The spherical core-shell form factor for coil-SGLCP diblock micelles is derived in Appendix D to be

$$\frac{1}{f_{PS}^2}P(q) = \left[V_c^2K_c\psi_c^2 + 2V_cV_sK_{cs}\psi_c\psi_s + V_s^2K_s\psi_s^2\right], \quad \text{(C.7)}$$

where

$$\psi_x = \frac{3[\sin(qR_x) - qR_x\cos(qR_x)]}{(qR_x)^3},$$

$$K_c = \left[(\rho_{PS} - \rho_{d_{19}5CB}) - \frac{v_{LCP}}{v_{PS}} \frac{R_c^3}{R_s^3 - R_c^3} (\rho_{LCP} - \rho_{d_{19}5CB}) \right]^2,$$

$$K_{cs} = \left[(\rho_{PS} - \rho_{d_{19}5CB}) - \frac{v_{LCP}}{v_{PS}} \frac{R_c^3}{R_s^3 - R_c^3} (\rho_{LCP} - \rho_{d_{19}5CB}) \right] \left[\frac{v_{LCP}}{v_{PS}} \frac{R_c^3}{R_s^3 - R_c^3} (\rho_{LCP} - \rho_{d_{19}5CB}) \right],$$

and

$$K_s = \left[\frac{v_{LCP}}{v_{PS}} \frac{R_c^3}{R_s^3 - R_c^3} (\rho_{LCP} - \rho_{d_{19}5CB}) \right]^2.$$

Equation C.7 contains only two adjustable parameters: R_c and R_s, the radius of the core and overall micelle, respectively (Figure C.1a). ρ_{PS}, ρ_{LCP}, and $\rho_{d_{19}5CB}$ denote the scattering length densities of pure PS, SGLCP, and $d_{19}5CB$, respectively, while v_{PS} and v_{LCP} denote the volumes of one polystyrene block and one SGLCP block, respectively. The scattering length densities are listed in Table D.1 and the polymer volumes are calculated from the molecular weights and the densities listed in Table D.1. Keeping the ratio of R_s / R_c constant, a Schultz distribution (Equation C.4) of core sizes is used to calculate the unsmeared intensity with Equation C.5 and Equation C.7, absorbing the volume fraction of PS in the core, f_{PS}, into a constant $K' = K / f_{PS}^2$. A Lorentzian describing the monomer-level scattering of a polymer with correlation length ξ is added to describe the high-q scattering:

$$I(q) = \frac{K_L}{\left(1 + (q\xi)^2\right)}, \tag{C.8}$$

where K_L is a weighting factor for this term. Equation C.8 was used to model scattering from SGLCP homopolymers in Chapter 5. The total intensity is smeared with the resolution function of the Small-Angle Scattering Instrument (SASI) at Argonne National Laboratory's Intense Pulsed Neutron Source, which has been previously reported[17] and is interpolated for numeric integration with a sixth degree polynomial (Figure C.2). In summary, the total calculated intensity is

$$I(q) = \frac{\int_0^\infty \left[\int_0^\infty n(R_c) K' P(q', R_c) dR_c + \frac{K_L}{\left(1 + (q'\xi)^2\right)} \right] \exp\left[-\frac{(q'-q)^2}{2\sigma(q)^2} \right] dq'}{\int_0^\infty \exp\left[-\frac{(q'-q)^2}{2\sigma(q)^2} \right] dq'} + I_{inc} \qquad \text{(C.9)}$$

with $K' = K / f_{PS}^2$, $n(R_c)$ given by Equation C.4, and $P(q, R_c)$ given by Equation C.7. I_{inc} accounts for q-independent background scattering. Least-squares fitting of Equation C.9 to the experimental scattering patterns is performed with WaveMetrics IGOR Pro® using procedures available from the NIST Center for Neutron Research,[18, 19] modified to include Equation C.7.

SANS patterns are well-described by Equation C.9 (Figure C.3), and the fits give values of R_c and R_s (Figure C.4 and Figure C.5). Least-squares fitting was initially performed allowing all the variables, K', R_c, R_s, β, K_L, ξ, and I_{inc}, to float freely. A second round of data fitting was performed at fixed polydispersities, $p = (1+\beta)^{-1/2}$. The quality of fit changes with p, but the values of R_c and R_s are insensitive to this parameter. Mean values of R_c and R_s (such as those reported in Figure C.4 and Figure C.5) are calculated by averaging R_c and R_s values obtained from fits with p fixed at various values between 0.01 and 0.45. The average is weighted by the sum of the square of the residuals, χ^2, between the fit and the experimental data.

C.1.3 Checking Fits for Self-Consistency and Physical Significance

The length scales extracted from fits to Equation C.9 must be checked for realism and self-consistency. The aggregation number, N_{agg}, is related to R_c and f_{PS} by

$$N_{agg} = \frac{f_{PS} \frac{4}{3} \pi R_c^3}{v_{PS}}, \qquad \text{(C.10)}$$

allowing an upper limit on N_{agg} to be estimated assuming the core is solvent-free ($f_{PS} = 1$). An upper limit on N_{agg} may also be estimated from the thickness of the shell, using the analogous relation,

$$N_{agg} = \frac{f_{LCP} \frac{4}{3} \pi \left(R_s^3 - R_c^3 \right)}{v_{LCP}}, \qquad \text{(C.11)}$$

and assuming the shell is solvent-free (f_{LCP} = 1). The upper limits on N_{agg} for 5 wt % diblock solutions in Figure C.4, estimated from Equations C.10 and C.11, jar the intuition (Table C.1). Qualtitative trends in the micelle sizes and aggregation numbers for 5 wt % diblock solutions are in agreement with the conclusions drawn from the raw data (Chapter 3). N_{agg} increases with the size of the PS block (Figure C.4) and decreases with increasing temperature (Figure C.5). However, the values of N_{agg} estimated for the core and corona are not consistent with one another. The corona is expected to be highly swollen with solvent, and the upper limit of N_{agg} estimated from Equation C.11 should, therefore, be much larger than that estimated from Equation C.10, but the data show the opposite trend: N_{agg} estimated from the shell dimension is, at most, 50% of that estimated from the core. In the physically unrealistic case that the corona is composed of pure SGLCP, these values of N_{agg} would require between 50 and 70% of the core's volume to be occupied by solvent (Table C.1). In a more realistic scenario, if the volume fraction of SGLCP in the shell is 0.5, the core would have to be composed of more than 70% solvent (Table C.1).

A fundamental assumption of the core-shell model may be responsible for the discrepancy between N_{agg} estimated from the core and the corona. In applying this model it was assumed that there is a well-defined interface between the surface of the micelle and a matrix composed of pure d_{19}5CB. In reality, one expects the volume fraction of SGLCP in the corona to decay with increasing distance from the core.[20-22] The high-density layer of polymer immediately adjacent to the core surface may constitute and effective shell in an effective matrix of SGLCP/d195CB solution; this phenomenon has been observed before in aqueous solutions of PEO-PPO-PEO micelles.[23] A better model for PS-SGLCP micelles may be a core-shell model with a density profile (Figure C.1e), but attempts to fit the data with such models fail because the selection of a functional form for the density decay is arbitrary and introduces additional fitting parameters.[9] Since equality of the aggregation number in the core and shell was imposed in deriving the form factor (Appendix D), the accuracy of R_c derived from the core-shell model relies on the accuracy of the shell thickness and both length scales are therefore suspect.

Confidence in the extracted length scales is further called into doubt by the observation that different form factors can provide equally good fits to the data (Figure C.6). The form factor for a homogenous cylinder with radius of 185 Å and length of 545 Å provides a description of data from 5 wt % 320(120)ABSiCB4 just as well as the spherical core-shell model. Without data from monodomain samples it is impossible to determine whether an anisotropic model is more appropriate for these micelles. Even if this were the case, models for elliptical core-shell structures are extremely difficult to fit because there are twice as many length scales involved (Figure C.1b).

C.1.4 Conclusions

SANS data from solutions of PS-SGLCP diblock copolymer micelles can be fit with a spherical core-shell model, but the length scales extracted from the fits are highly suspect. The corresponding aggregation numbers estimated for the core and shell are inconsistent with one another and the radial density profile of SGLCP in the corona that likely exists is not considered at all by the model. Furthermore, it is unknown whether a spherical model is even appropriate for these micelles; the orientation of the LC solvent probably causes them to adopt anisotropic forms.[24, 25]

The limited range of scattering vectors is, perhaps, the biggest obstacle standing in the way of extracting meaningful length scales from this data. The size of these micelles is greater than 150 Å according to every form factor that was attempted. To get unambiguous fits to a form factor, plenty of data should be available in a range of $q < L^{-1}$, where L is the characteristic length scale. The minimum value of q that was accessed in these experiments is 0.00666 $Å^{-1}$, giving q *equal* to L^{-1} at best. Perhaps data fitting would be more successful if the experiments were repeated at a facility giving access to lower values of q (e.g., the NIST Center for Neutron Research or, perhaps, a small-angle x-ray scattering beamline).

C.2 Tables

Table C.1 Upper bounds on the aggregation number (N_{agg}) in 5 wt % solutions of diblock copolymers estimated from the size of the core using Equation C.10 and from the size of the shell using Equation C.11. The volume fraction of polystyrene in the core (f_{PS}) is estimated from N_{agg} of the shell for two cases: a shell composed of pure SGLCP (f_{LCP} = 1.0) and a shell composed of 50% SGLCP and 50% solvent (f_{LCP} = 0.5).

Polymer	Max N_{agg} (core)	Max N_{agg} (shell)	f_{PS} (f_{LCP} = 1.0)	f_{PS} (f_{LCP} = 0.5)
470(40)ABSiCB4	210	58	0.52	0.14
390(60)ABSiCB4	240	95	0.34	0.20
420(80)ABSiCB4	2200	760	0.40	0.17
320(120)ABSiCB4	4200	2200	0.27	0.26

C.3 Figures

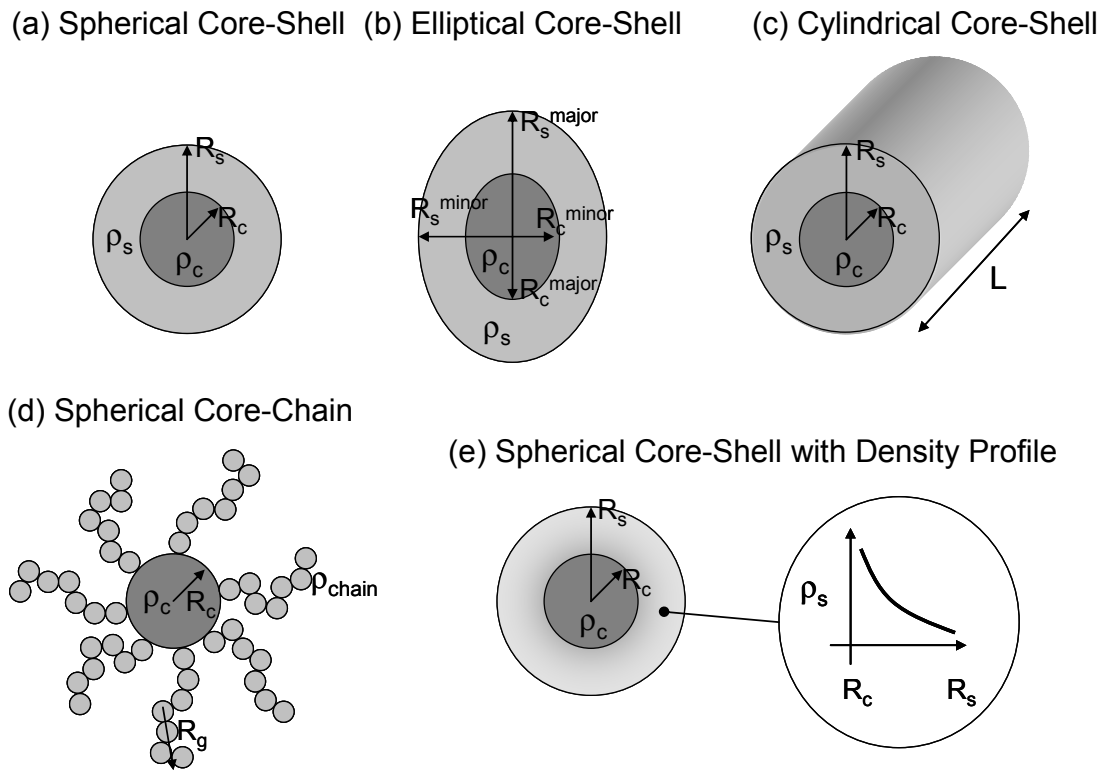

Figure C.1 Schematic drawings of examples of structural models that may be used to calculate form factors of block copolymer micelles. These examples all assume a core of radius R_c with homogenous neutron scattering length density, ρ_c. (a,b,c,e) The core-shell models assume the core is surrounded by a concentric shell with scattering length density ρ_s such that the overall micelle's radius is R_s. (d) In the core-chain model, the core is surrounded by a corona of polymer chains having neutron scattering length density ρ_{chain} and radii of gyration R_g.

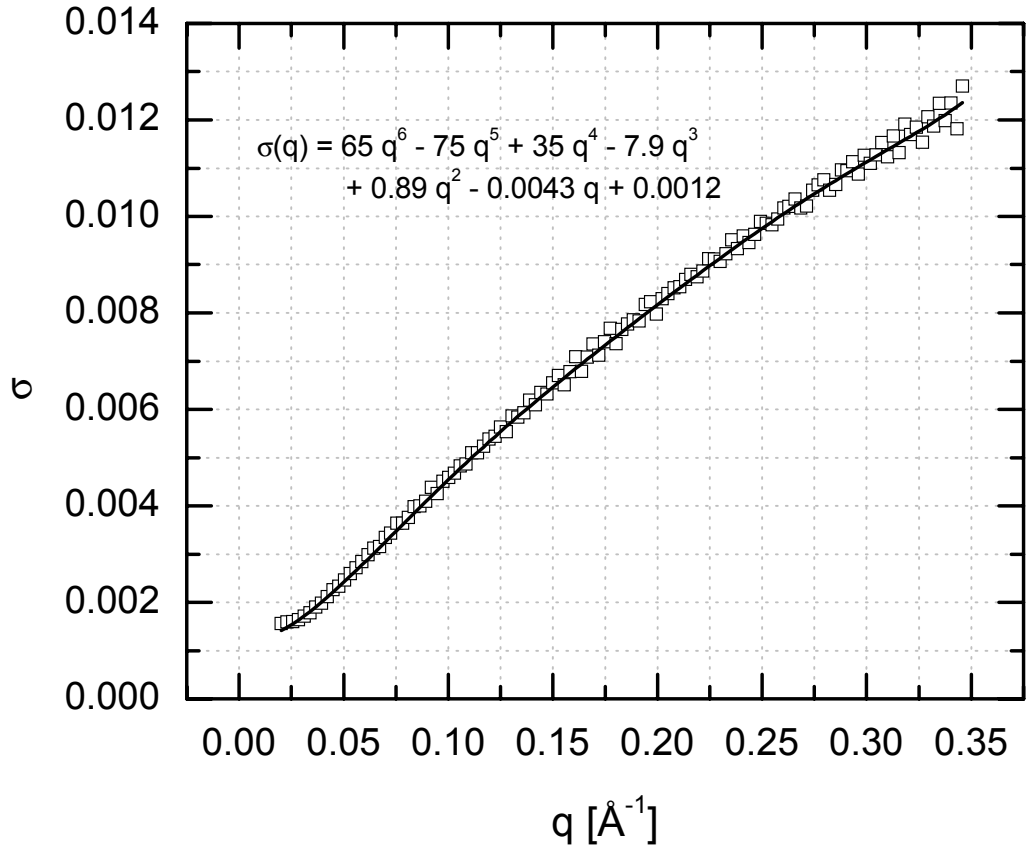

Figure C.2 Resolution function of the Small-Angle Scattering Instrument (SASI) at Argonne National Laboratory's Intense Pulsed Neutron Source. Experimentally determined[17] values of σ (square symbols) were interpolated with a sixth degree polynomial (line).

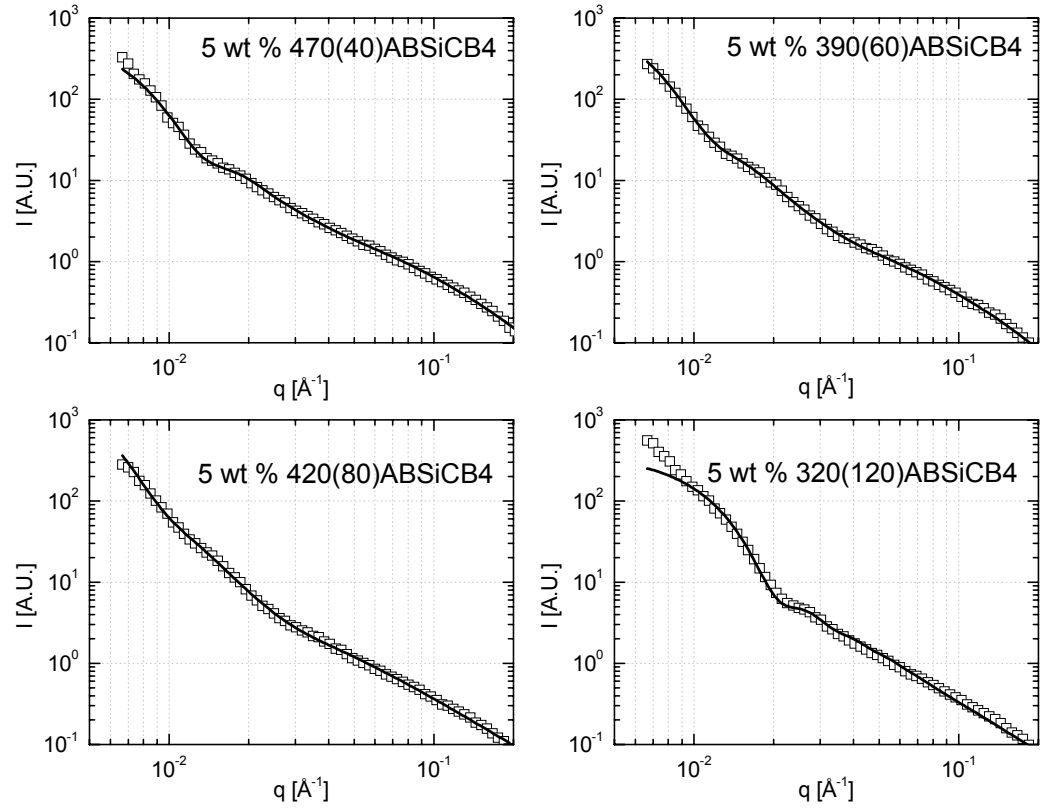

Figure C.3 Small-angle neutron scattering data from 5 wt % diblock copolymer solutions at 25 °C (square symbols) together with representative fits (lines) obtained using the spherical core-shell form factor (Equation D.9).

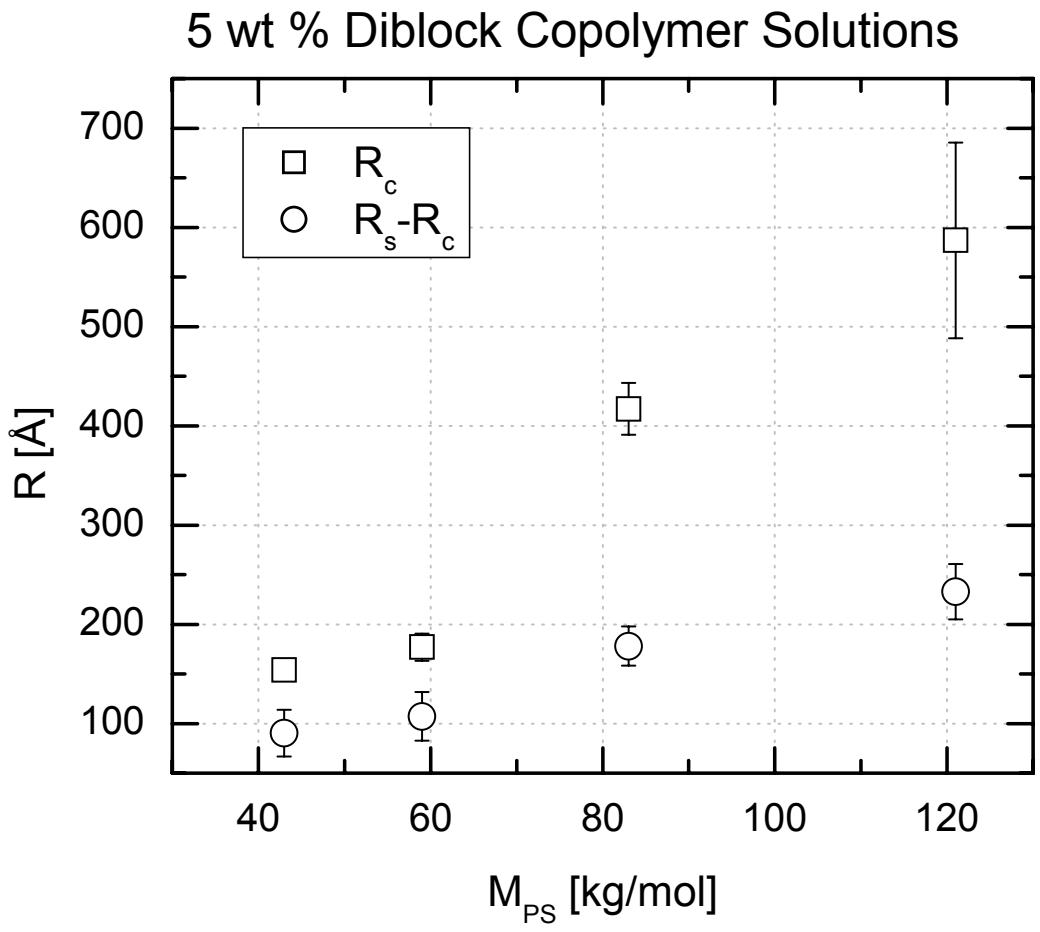

Figure C.4 Values of the core radius (R_c) and shell thickness (R_s - R_c) for 5 wt % solutions of 470(40)ABSiCB4, 390(60)ABSiCB4, 420(80)ABSiCB4, and 320(120)ABSiCB4 at 25 °C as a function of the molecular weight of the polystyrene block (M_{PS}). Values are derived from fitting neutron scattering data to the spherical core-shell model (Equation D.9). Error bars represent the standard deviation of an average from fits using different polydispersities, weighted by the fits' χ^2.

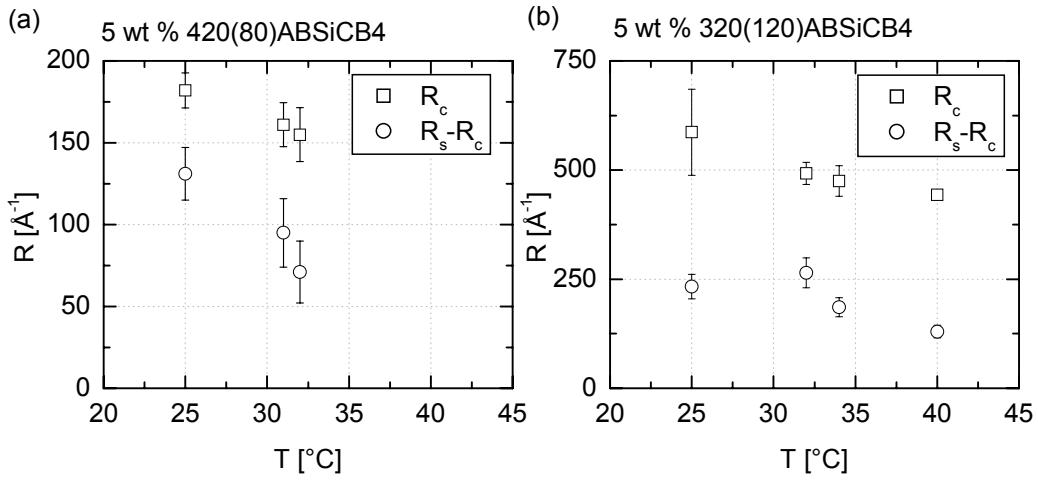

Figure C.5 Values of the core radius (R_c) and shell thickness (R_s - R_c) for (a) 5 wt % 420(80)ABSiCB4 and (b) 5 wt % 320(120)ABSiCB4 as a function of temperature. Values are derived from fitting neutron scattering data to the spherical core-shell model (Equation D.9). Error bars represent the standard deviation of an average from fits using different polydispersities, weighted by the fits' χ^2.

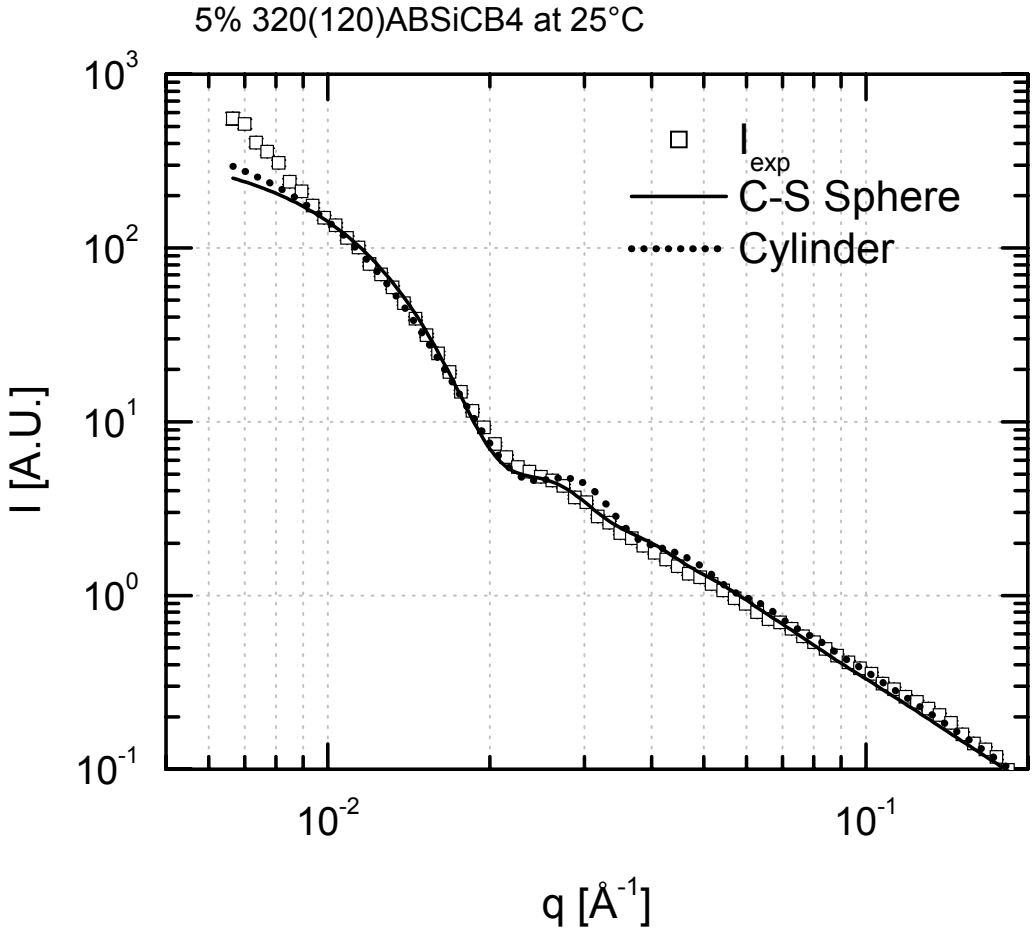

Figure C.6 Small-angle neutron scattering data from 5 wt % 320(120)ABSiCB4 at 25 °C (I_{exp}) shown together with a representative fit using the spherical core-shell model (Equation D.9) and the form factor for a cylinder of homogeneous scattering length density.

C.4 References

[1] Glatter, O.; Kratky, O., eds. *Small Angle X-Ray Scattering*. 1982, Academic Press: London.

[2] Higgins, J. S.; Benoit, H. C. *Polymers and Neutron Scattering*, Oxford Series on Neutron Scattering in Condensed Matter, ed. S.W. Lovesey; E.W.J. Mitchell; Oxford University Press: New York, NY, 1996.

[3] Kotlarchyk, M.; Chen, S.-H. Analysis of small angle neutron scattering spectra from polydisperse interacting colloids. *J. Chem. Phys.* **1983**, *79*, 2461-2469.

[4] King, S. M.; Griffiths, P. C.; Cosgrove, T. Using SANS to Study Adsorbed Layers in Colloidal Dispersions. In *Applications of Neutron Scattering to Soft Condensed Matter*; B.J. Gabrys, Editor; Gordon and Breach Science Publishers: Amsterdam, 2000.

[5] Pedersen, J. S. Analysis of small-angle scattering data from colloids and polymer solutions: modeling and least-squares fitting. *Adv. Colloid Interface Sci.* **1997**, *70*, 171-210.

[6] Pedersen, J. S.; Gerstenberg, M. C. Scattering Form Factor of Block Copolymer Micelles. *Macromolecules* **1996**, *29*, 1363-1365.

[7] Svaneborg, C.; Pedersen, J. S. Form Factors of Block Copolymer Micelles with Excluded-Volume Interactions of the Corona Chains Determined by Monte Carlo Simulations. *Macromolecules* **2002**, *35*, 1028-1037.

[8] Castelletto, V.; Hamley, I. W.; Pedersen, J. S. A small-angle neutron scattering investigation of the structure of highly swollen block copolymer micelles. *J. Chem. Phys.* **2002**, *117*, 8124-8129.

[9] Pedersen, J. S.; Svaneborg, C.; Almdal, K.; Hamley, I. W.; Young, R. N. A Small-Angle Neutron and X-ray Contrast Variation Scattering Study of the Structure of Block Copolymer Micelles: Corona Shape and Excluded Volume Interactions. *Macromolecules* **2003**, *36*, 416-433.

[10] Bang, J.; Viswanathan, K.; Lodge, T. P.; Park, M. J.; Char, K. Temperature-dependent micellar structures in poly(styrene-b-isoprene) diblock copolymer solutions near the critical micelle temperature. *J. Chem. Phys.* **2004**, *121*, 11489-11500.

[11] Pedersen, J. S. Form factors of block copolymer micelles with spherical, ellipsoidal and cylindrical cores. *J. Appl. Crystallogr.* **2000**, *33*, 637-640.

[12] Kinning, D. J.; Thomas, E. L. Hard-Sphere Interactions between Spherical Domains in Diblock Copolymers. *Macromolecules* **1984**, *17*, 1712-1718.

[13] Percus, J. K.; Yevick, G. J. Analysis of Classical Statistical Mechanics by Means of Collective Coordinates. *Phys. Rev.* **1958**, *110*, 1-13.

[14] Castelletto, V.; Hamley, I. W. Small-Angle Neutron Scattering Study of the Structure of Superswollen Micelles Formed by a Highly Asymmetric Poly(oxybutylene)-Poly(oxyethylene) Diblock Copolymer in Aqueous Solution. *Langmuir* **2004**, *20*, 2992-2994.

[15] Wignall, G. D.; Christen, D. K.; Ramakrishnan, V. Instrumental Resolution Effects in Small-Angle Neutron Scatterin. *J. Appl. Crystallogr.* **1988**, *21*, 438-451.

[16] Scruggs, N. R.; Kornfield, J. A.; Lal, J. Using the "Switchable" Quality of Liquid Crystal Solvents to Mediate Segregation between Coil and Liquid-Crystalline Polymers. *Macromolecules* **2006**, *39*, 3921-3926.

[17] Thiyagarajan, P.; Epperson, J. E.; Crawford, R. K.; Carpenter, J. M.; Klippert, T. E.; Wozniak, D. G. The Time-of-Flight Small-Angle Neutron Diffractometer (SAD) at IPNS, Argonne National Laboratory. *J. Appl. Crystallogr.* **1997**, *30*, 280-293.

[18] NIST Center for Neutron Research. *NCNR tools on the web, http://www.ncnr.nist.gov/resources/index.html*. June 30, 2003 [cited November 8 2006].

[19] NIST Center for Neutron Research. *SANS and USANS Data Reduction and Analysis with IGOR Pro, http://www.ncnr.nist.gov/programs/sans/data/red_anal.html*. August 17, 2006 [cited November 8 2006].

[20] Halperin, A. Polymeric Micelles: A Star Model. *Macromolecules* **1987**, *20*, 2943-2946.

[21] Halperin, A.; Tirrell, M.; Lodge, T. P. Tethered Chains in Polymer Microstructures. *Adv. Polym. Sci.* **1992**, *100*, 31-71.

[22] Milner, S. T. Polymer Brushes. *Science* **1991**, *251*, 905-914.

[23] Mortensen, K.; Pedersen, J. S. Structural Study of the Micelle Formation of Poly(ethylene oxide)-Poly(propylene oxide)-Poly(ethylene oxide) Triblock Copolymer in Aqueous Solution. *Macromolecules* **1993**, *26*, 805-812.

[24] Walther, M.; Bohnert, R.; Derow, S.; Finkelmann, H. Structure formation of liquid-crystalline isotropic AB block copolymers in nematic solvents. *Macromol. Rapid Commun.* **1995**, *16*, 621-629.

[25] Walther, M.; Faulhammer, H.; Finkelmann, H. On the thread-like morphology of LC/I block copolymers in nematic solvents. *Macromol. Chem. Phys.* **1998**, *199*, 223-237.